Available online at www.sciencedirect.com
SCIENCE DIRECT
International Journal of Heat and Mass Transfer 49 (2006) 4095–4105
International Journal of HEAT and MASS TRANSFER
www.elsevier.com/locate/ijhmt

The effective thermal conductivity of wire screen

Chen Li, G.P. Peterson *

Rensselaer Polytechnic Institute, Department of Mechanical, Aerospace and Nuclear Engineering, 110, 8th Street, Troy, NY 12180, United States

Received 17 November 2005; received in revised form 22 March 2006
Available online 27 June 2006

Abstract

A combined experimental and theoretical investigation was conducted to examine the thermal conductivity of layers of wire mesh screen. Employing a carefully controlled sintering process, layers of sintered wire screen were examined experimentally. The experimental results indicate that the effective thermal conductivity in the *z*-direction (i.e., normal to the plane of the wire screen layers) for single layer, inline structures and staggered multilayer wire screens is approximately 4–25% and 6.4–35% times that of the solid metal thermal conductivity, respectively. In addition to the conductivity of the base material, the contact conditions between the individual wires, as well as between the individual layers were found to be the most important factors in the determination of the effective thermal conductivity. In parallel with the experimental investigation, an analytical model was developed and shown to accurately predict the effective thermal conductivity of these layers as a function of the contact conditions between the wires, between the individual layers, and between the solid heating surface and the first layer of screen. In addition to the contact conditions, this new model is strongly dependent on three geometric parameters: the mesh number, M, the wire diameter, d, and the compression factor, cf. Experimental data from this and other investigations were used to verify the accuracy of the model, which was shown to accurately predict the effective conductivity as a function of the above mentioned parameters. In addition, a comprehensive literature review was performed and analyzed in order to further substantiate the validity and accuracy of this new model. The resulting conclusions highlight the importance of the contact conditions between the wires in the individual layers, and between the layers and the solid surface.

Keywords: Effective thermal conductivity; Volumetric porosity; Wire screen; Contact condition

1. Introduction

Due to the ease of fabrication and high degree of accuracy with which the various parameters, such as volumetric porosity, ε, and specific surface area, β, can be controlled, layers of sintered wire screen are often used in commercial applications to provide enhanced heat transfer or capillary assisted reflow in two-phase systems [1–14]. These layers of wire screen are routinely used in numerous applications such as porous fins, capillary wick structures in heat pipes, filling materials and regenerators for Stirling engines, and many other applications. In many of these applications, it is often important to understand and improve the effective thermal conductivity and/or control the volumetric porosity, as well as the specific surface area in order to enhance the overall heat transfer performance. A number of investigators have successfully developed wire mesh based porous media with highly effective thermal conductivities. Xu and Wirtz [2] developed plain-woven screen laminates with highly effective thermal conductivities in the wire length direction, i.e., in the x-direction, by soldering the layers of the wire screen together. Tye [7] fabricated 304L stainless steel "Rigimesh" and experimentally studied the parameters that affect its thermal conductivity. In this investigation, the effective thermal conductivity was found to vary from 4.3 to 25.4 W/mK depending upon the volumetric porosity and was further shown to increase with increasing temperature.

Generally the effective thermal conductivity of wire mesh in the z-direction is strongly related to the fabrication

* Corresponding author. Tel: +1 518 276 6487; fax: +1 518 276 4061.
E-mail address: peterson@rpi.edu (G.P. Peterson).

0017-9310/$ - see front matter © 2006 Elsevier Ltd. All rights reserved.
doi:10.1016/j.ijheatmasstransfer.2006.03.031

Nomenclature

a	length of the cross-sectional area of the wire in the x-direction (m) in Eq. (9)
A	dimensionless parameter defined by d/w
B	dimensionless parameter defined by d/t
b	length of the cross-sectional area of the wire in the z-direction (m) in Eq. (9)
C	coefficient in Eq. (6)
c	length of one side of the contact area (m) in Eq. (9)
cf	compression factor
D	wire diameter (m)
K	thermal conductivity (W/mK)
K_{fs}	non-dimensional thermal conductivity defined by K_f/K_s
K_{es}	non-dimensional thermal conductivity defined by K_{eff}/K_s
l_x, l_y, l_z	spacing of the wires in the x, y, and z-directions, respectively (m)
M	mesh number
Md	dimensionless parameter defined by $M \times d$
n	number
q''	heat flux (W/m^2)
S	crimping factor
t	thickness (m)
T	temperature (K)
ΔT	temperature difference (K)
w	the opening width of wire screen (mm)

Greek symbols

α	empirical constant in Eq. (4)
γ_{ax}, γ_{ay}, γ_{az}	a/l_x, a/l_y, b/l_z, respectively in Eq. (8,9)
γ_c	c/a in Eq. (8,9)
ε	volumetric porosity

Subscripts

1, 2, and 3	section number in the unit cell
Cu	parameter related solid copper bar
c1–c4	thermocouple number in the cooling side
e	dimensionless effective parameter
eff	effective parameter
ex, ey, ez	effective parameter in the three principle directions
es	effective parameter/parameter in solid phase
fs	parameter in fluid phase/parameter in solid phase
f	fluid phase
hole	holes on the copper bar for the thermocouples
h1–h4	thermocouple number on the heating side
layer	parameter related to the wire screen layer
S	solid phase
s1 and s2	thermocouple number on the sample
Lower	parameter for the lower limit
Upper	parameter for the upper limit
w	parameter related to the wire screen
X, x	x-coordinate
Y, y	y-coordinate
Z, z	z-coordinate

process, i.e., wrapped, sintered or soldered. Previous investigations, which are later summarized in the literature review, have indicated that the contact conditions between the wires as well as between the individual layers are the determining factor in the effective thermal conductivity of the wire screen, and the accurate prediction of the effective thermal conductivity is strongly dependent on the understanding of the contact conditions. In the current investigation, layers of copper wire screens were utilized along with an optimized sintering process developed by Li et al. [3] to achieve nearly perfect contact conditions between the individual copper wires, both within the individual layers and also between the respective layers. The objectives of the current investigation are to develop a porous media based on layers of wire screen and to predict and measure the magnitude of the effective thermal conductivity in the z-direction for this type of porous media. A theoretical model that can accurately predict the effective thermal conductivity in the z-direction, is developed, as a function of the dimensionless parameter, Md; the compression factor, cf; the thermal properties of the wire mesh and the fluid; as well as contact conditions between the individual wires and between the first screen layer and the heated surface. Tests were conducted to experimentally verify the accuracy of this new analytical model, by measuring the effective thermal conductivity of the wire mesh. The experimental procedure is described in detail and both the experimental data and the results of the analytical model are compared with previous analytical and experimental data available in the literature.

2. Literature review

2.1. Existing models of effective thermal conductivity of wire screen

The most frequently used correlation for predicting the effective thermal conductivity of a single layer of wire mesh was first proposed by Rayleigh [1] and is given in Eq. (1). This analytical expression has been widely used in the design of fluid-saturated screen wicks in heat pipes and other industrial applications. In the development of this expression, Rayleigh assumed that the porous material is isotropic. Comparison with experimental data, however, has demonstrated that this approach is not capable of accurately predicting the effective thermal conductivity of layers of screen mesh [9].

$$K_{\mathrm{eff}} = \frac{K_{\mathrm{f}}[K_{\mathrm{f}} + K_{\mathrm{s}} - (1-\varepsilon)(K_{\mathrm{f}} - K_{\mathrm{s}})]}{K_{\mathrm{f}} + K_{\mathrm{s}} + (1-\varepsilon)(K_{\mathrm{f}} - K_{\mathrm{s}})} \tag{1}$$

The primary reason for the disparity between the measured and predicted values is the failure to accurately incorporate the effect of the contact conditions between the wires and/or between the wires and the solid surface.

Based on previously developed experimental data, Alexander [4] developed an empirical model for the effective conductivity of layers of sintered wire screens in the z-direction, when saturated with either air or water as:

$$K_{\mathrm{eff}} = K_{\mathrm{f}}(K_{\mathrm{s}}/K_{\mathrm{f}})^{(1-\varepsilon)^{0.59}} \tag{2}$$

Koh and Fortini [5] expanded an expression derived by Aivazov and Domashnev [6], and developed an empirical correlation for the prediction of the effective thermal conductivity of sintered stainless steel mesh screen, i.e., "Regimesh", based on the experimental data measured by Tye [7]. This correlation, in which the thermal conductivity of the saturated fluid is neglected, is shown below as Eq. (3).

$$K_{\mathrm{eff}} = \frac{1-\varepsilon}{1+11\varepsilon}K_{\mathrm{s}} \tag{3}$$

Chang [8] utilized a somewhat different approach by transforming the screen into layered, rectangular cross-sectional segments and utilized an analysis of the combined thermal resistances in series and parallel arrangements. Based on this analysis and the definition of a unit cell, mathematical models of the effective thermal conductivity in the z-direction and the volumetric porosity of the wire screen were proposed. In these models, the contact conditions between the individual metal filaments were carefully considered and were denoted by the parameter, α. Eq. (4) was then developed for a single layer of screen, but was also found to be applicable to multiple layers of screen mesh material:

$$K_{\mathrm{eff}} = \frac{K_{\mathrm{f}}}{(1+A)^2}\left\{\alpha^2 A\left[\frac{\alpha A}{\alpha - \pi B(1-K_{\mathrm{f}}/K_{\mathrm{s}})/2} + \frac{2[1+A(1-\alpha)]}{\alpha - \pi B(1-K_{\mathrm{f}}/K_{\mathrm{s}})/4}\right] + [1+A(1-\alpha)^2]\right\} \tag{4}$$

where $A = d/w$, $B = d/t$, d is the wire diameter, w is the opening width of the mesh, and t is the thickness of a single layer of wire screen. For the case of multiple layers, $t = t_w/n_{\mathrm{layer}}$. The range of α is defined by Eq. (5):

$$\pi d/(2t) \leqslant \alpha \leqslant 1 + w/d \tag{5}$$

Based upon comparisons with previous analytical models and the test data available in the literature, this model was found to be capable of predicting the effective thermal conductivity for specific values of α, when the ratio $K_{\mathrm{s}}/K_{\mathrm{f}}$ ranged from 25 to 160 reasonably, but correlated rather poorly when the ratio was greater than 600. For single layers of wire screen, the thickness, t, is normally equal to twice the wire diameter, d, or $t = 2d$. From Eq. (4), the lower limit of α is $\pi/4$. Based on Eq. (4), for copper wire screen with a mesh number of $3.937 \times 10^3\ \mathrm{m}^{-1}$ ($100\ \mathrm{in}^{-1}$) and $d = 0.1143$ mm, when $\alpha = \pi/4$, i.e., the metal wires will have a direct contact area, K_{eff}, of approximately 49.6 W/mK with air as the fluid. However, when $\alpha = 1$, i.e, there is a gap of approximately 50 μm between the metal wires, the value of K_{eff} is reduced to 0.05 W/mK. This simple case study clearly illustrates how important the contact conditions between the metal wires are in the determination of the effective thermal conductivity of layers of wire screen in the z-direction.

Xu and Wirtz [2] developed a new type of isotropic screen laminate by bonding and stacking plain-woven copper screens and them together using 95/5 Sn/Antimony solder. Following the method of Chang [8], Xu and Wirtz [2] also established a transformed unit cell, and derived physical models to predict the in-plane effective thermal conductivity along the wire length direction of the bonded screen laminate, i.e., the x-direction as given in Eq. (6). The study of Xu and Wirtz [2] indicated that the effective conductivity ranged from 23% and 78% of the conductivity of the filament material for isotropic and anisotropic plain-weave screen laminates, respectively. Because the wires were bonded with a high conductivity solder material, the metal filaments were assumed to have very good contact conditions. The K_{eff} of the bonded wire screen along wire directions was found to be as high as 105 W/mK for isotropic copper wire screen and air. An experimental investigation was also conducted to benchmark the physical models, which illustrated good agreement with the test data.

$$\mathrm{cf} \cdot K_{\mathrm{es}} = \frac{80\pi \cdot Md \cdot (K_{\mathrm{fs}} - 1) + C \cdot \mathrm{cf} \cdot K_{\mathrm{fs}}}{C} + \frac{C \cdot \mathrm{cf}^2 \cdot K_{\mathrm{fs}}}{320\pi \cdot Md \cdot (1 - K_{\mathrm{fs}}) + 2C \cdot \mathrm{cf}} \tag{6}$$

$$\mathrm{cf}[1-\varepsilon] = -3.906 \times 10^{-4}\pi \cdot C \cdot Md \tag{7}$$

where $C = 123Md^4 - 384Md^2 - 640$, M is the mesh number, d is the wire diameter, cf is the compression factor defined by $t/(n_{\mathrm{layer}} \cdot 2d)$, and the K_{es} is the non-dimensional effective thermal conductivity defined by $K_{\mathrm{eff}}/K_{\mathrm{s}}$.

Hsu et al. [9] obtained algebraic expressions for the effective thermal conductivity of wire screen in the three principle directions: x, y and z, based on a lumped parameter method. In this investigation, the contact resistance between the wires was incorporated through a parameter, γ_c, and was used to estimate the contact area between the wires. The effective thermal conductivity of the wire screens in the x-direction was defined as

$$\frac{K_{\mathrm{ex}}}{K_{\mathrm{f}}} = [1 - \gamma_{ay}\gamma_{by} - \gamma_{bz} - \gamma_{ay}\gamma_c(1-2\gamma_{bz})] + \frac{\gamma_{ay}\gamma_{bz}}{K_{\mathrm{fs}}} + \frac{\gamma_{bz}}{\gamma_{ax}(K_{\mathrm{fs}} - 1) + 1} + \frac{\gamma_{ay}\gamma_c(1-2\gamma_{bz})}{\gamma_{ax}\gamma_c(K_{\mathrm{fs}} - 1) + 1} \tag{8}$$

The expression for K_{ey} in the y-direction was obtained by interchanging γ_{ay} and γ_{ax} in Eq. (8). For isotropic wire screen, these terms are identical. Eq. (9) presents the resulting expression for K_{ez}.

$$\frac{K_{ez}}{K_f} = (1-\gamma_{ay})(1-\gamma_{ax}) + \frac{\gamma_{ax}+\gamma_{ay}-2\gamma_{ax}\gamma_{ay}}{\gamma_{bz}(K_{fs}-1)+1} + \frac{\gamma_{ax}\gamma_{ay}(1-\gamma_c^2)}{2\gamma_{bz}(K_{fs}-1)+1} + \frac{\gamma_c^2\gamma_{ax}\gamma_{ay}}{K_{fs}} \quad (9)$$

In Eqs. (8) and (9), K_{fs} is defined as K_f/K_s; γ_{ax}, γ_{ay} and γ_{az} are a/l_x, a/l_y and a/l_z, respectively; l_x, l_y and l_y are the spacing of the wires in the x, y, and z-direction, respectively, and $\gamma_c = c/a$.

From an ideal and purely physical perspective a parallel arrangement offers the least thermal resistance to heat flow, while a series arrangement results in the greatest resistance, and the upper and lower limits can be defined by the equations for perfect parallel and series cases, respectively.

$$K_{upper} = \varepsilon K_f + (1-\varepsilon)K_s \quad (10)$$

$$K_{lower} = \left[\frac{\varepsilon}{K_f} + \frac{(1-\varepsilon)}{K_s}\right]^{-1} \quad (11)$$

2.2. Existing models of volumetric porosity of wire mesh

The porosity of a sample can be measured using the density method and the mesh number M, is defined as

$$M = 1/(d+w) \quad (12)$$

where d and w denote the wire diameter and the opening width of mesh, respectively. Chang [8] summarized the existing correlations for the porosity of wire mesh and by ignoring the degree of intermeshing between adjacent layers, Marcus [11] proposed Eq. (13)

$$\varepsilon = 1 - \pi SMd/4 \quad (13)$$

to predict the volumetric porosity, where S is the crimping factor, which is assumed to be approximately 1.05. The Engineering Sciences Data Unit (EDSU) in London [12] suggested a simpler correlation to estimate the porosity of single layers of wire mesh as

$$\varepsilon = 1 - \pi Md/4 \quad (14)$$

Armour and Cannon [13] presented a comprehensive model to predict the porosity of various types of screens as

$$\varepsilon = 1 - \frac{\pi AB}{2(A+B)}\sqrt{1+\left(\frac{A}{1+A}\right)^2} \quad (15)$$

where $A = d/w$, $B = d/t$, and t is the thickness of the wire mesh. The most recent method for predicting the volumetric porosity of wire screens was developed by Xu and Wirtz [2], and is shown as Eq. (7) above.

2.3. Results and discussion

2.3.1. Effective thermal conductivity

In the current investigation, copper wire screen and air were selected as the solid metal filament and fluid, respectively. Extensive case studies of the existing models and data were performed to systematically examine the reported values and predictive methods for the effective thermal conductivity of isotropic copper wire screen in both the x- and z-directions. Detailed information about the various cases is listed in Table 1. A total of 13 cases, which cover all existing models and the typical cases studied in these models, were evaluated and analyzed. Results of the various cases studied are illustrated and presented in Fig. 1. As shown in this figure, the existing models for K_{eff} can be reasonably categorized into two groups: (1) high effective thermal conductivity predictions, resulting from relatively good contact conditions between the wires; and (2) low effective thermal conductivity predictions resulting from poor contact conditions between the wires.

For the effective thermal conductivity of wire screen in the x-direction, the model of Xu and Wirtz [2] considered two types of wire screen structures: inline stacked (cf = 1) and staggered (cf < 1). The resulting models, indicated

Table 1
List of cases for isotropic wire screen

Case #	Model (year), Eq. #	Parameter presented contact area between wires	Contact area between wires	Remarks
1	Rayleigh [1], Eq. (1)	N/A	0	
2	Alexander [4], Eq. (2)	N/A	N/A	Empirical correlation
3	Chang [8], Eq. (4)	$\alpha = 0.5$	0	
4		$\alpha = 1$	0	
5		$\alpha = \pi/4$	$\pi^2 d^2/64$	
6	Hsu et al. [9], Eq. (8)	$\gamma_c = 0.1$	$\pi d^2/400$	
7		$\gamma_c = 1$	$\pi d^2/4$	
8	Hsu et al. [9], Eq. (9)	γ_c in x-direction, i.e., along wire length direction		K_e is not sensitive to this parameter
9	Xu and Wirtz [2], Eq. (6)	N/A, in x-direction	$\pi^2 d^2/64$	cf = 1, inline or single layer
10		N/A, in x-direction	$\pi^2 d^2/64$	cf = 0.7, staggered layers
11	Koh and Fortini [5], Eq. (3)	N/A	N/A	Empirical correlation
12	Upper limit, Eq. (10)	N/A	N/A	Parallel
13	Lower limit, Eq. (11)	N/A	N/A	Series

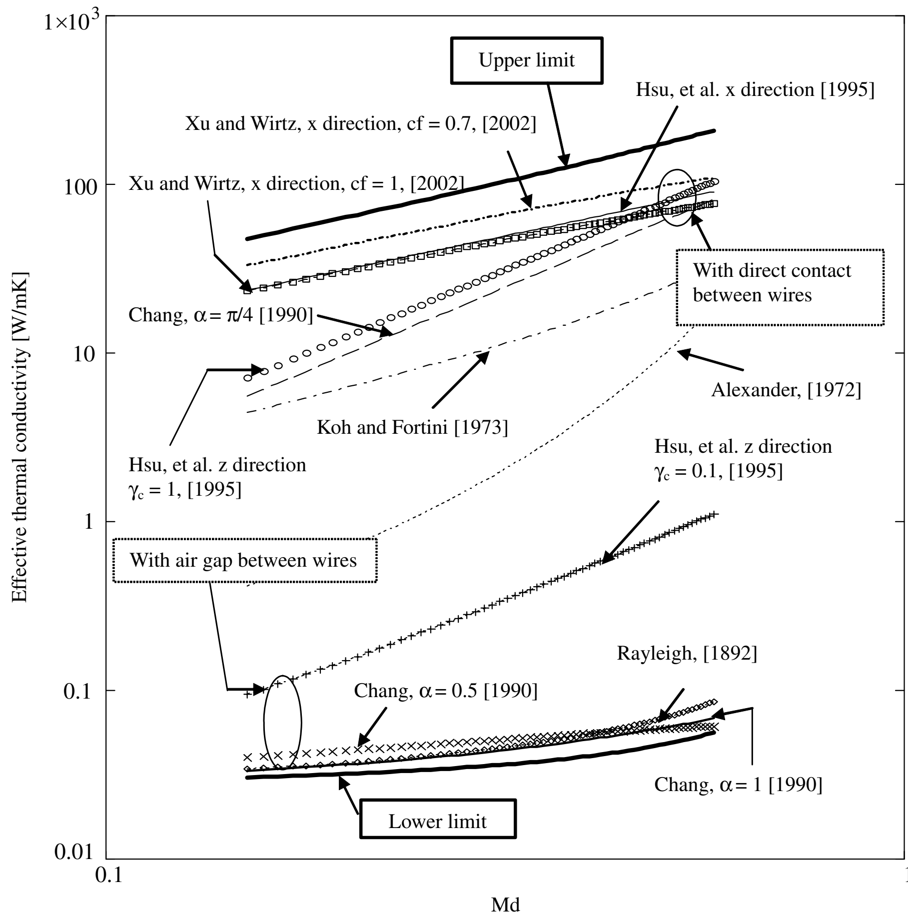

Fig. 1. Predictions of the effective thermal conductivity of wire screen from existing models.

good agreement with the model developed by Hsu et al. [9] for single layers or inline stacked structures in the *x*-direction. The model developed by Hsu et al., also indicated that the effective thermal conductivity of wire screens along the wire length direction was not very sensitive to the contact conditions between the wires.

Chang [8] and Hsu et al. [9] derived models to predict the effective thermal conductivity of wire screen in the *z*-direction. When the wires were in good contact with each other, the results were in good agreement, with the difference between the models caused primarily by the variations in the contact area between the wires, which are shown as cases 4 and 7 in Table 1. However, when there was no direct contact or only limited contact area between the wires, the existing models predicted very low values for the effective thermal conductivity and resulted in significant deviations from the predicted values. This difference is primarily caused by the uncertainties associated with the contact conditions between the wires or between the wire mesh and the heated surface. The empirical correlation of Alexander [4] provided a value that is in the mid-range of the predicted values. In this analysis, the sintered wire screens were clamped between two stainless steel surfaces, which may have resulted in a reasonably low contact thermal resistance between the wire mesh and the stainless steel surfaces. By considering the contact issues Tye [7] reported much higher effective thermal conductivities of layers of wire screen. These data were empirically correlated as Eq. (3) by Koh and Fortini [5].

Based upon this review, it is apparent that the contact conditions between the wires, as well as between the wire mesh and the heated surface, play a critical role in determining the overall thermal conductivity of the wire screen, K_{eff}, and moreover, when the wires are in good contact with each other, the thermal conductivity of the wire is the dominant factor in the determination of K_{eff}. If the quality of the thermal contact between the wires and layers is considered and/or incorporated, very high effective thermal conductivities can be achieved. Regardless of the quality of the actual contact conditions between the wire screens, as well as between the wire screen and the heating/cooling surfaces, in order to obtain accurate predictive techniques and understand the experimental data, careful attention must be given to these contact conditions.

2.3.2. The volumetric porosity

The results of the predictive models described in Section 2.2 and the experimental tests [4,13,14] are illustrated and compared in Fig. 2 as a function of the dimensionless parameter, *Md*, which describes the geometry of the wire

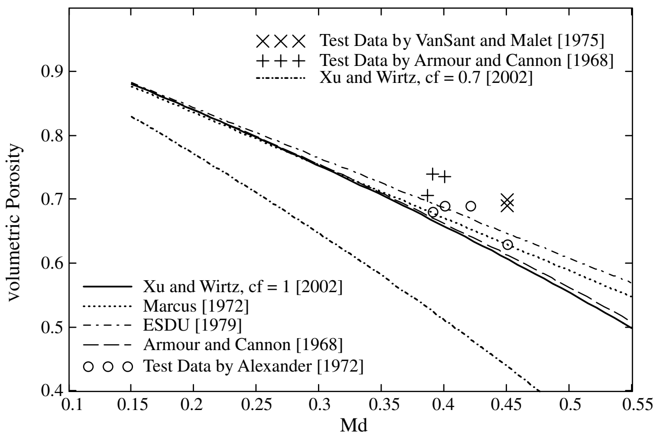

Fig. 2. Predictions and test data of the volumetric porosity of wire screen, presented as function of *Md*.

screen. Generally speaking, these models have better agreement for low values of *Md* than for higher values. In this comparison, only the model of Xu and Wirtz [2] considered the compression factor in the prediction of the multilayer case.

For single layers, either inline or stacked, the model of Xu and Wirtz [2] is consistent with the model of Armour and Cannon [13], and the data of Alexander shows relatively good agreement with the results predicted by the model of Marcus [11]. It is important to note that the existing experimental data have a narrow range of Md and a majority of the data available are greater than the values predicted by all of the existing models.

3. Test article fabrication

Isotropic copper wire screen was selected to benchmark the new and existing models. The optimized sintering process developed by Li et al. [3] was employed during the fabrication process in order to significantly reduce or even eliminate the effects of the thermal contact resistance between the wires as well as between the copper wire screen and the heating/cooling surfaces. A sintering temperature of 1030 °C in a gas mixture consisting of 75% argon and 25% hydrogen for a time of 2 h, was found to provide the optimal conditions for reducing the contact resistance for the copper materials utilized in the current investigation. SEM pictures were taken to evaluate the quality of the contacts and identify any differences in the contact conditions between the copper wires at different sintering temperatures. As shown in Figs. 3(a) and (b), these images clearly demonstrate that the contact between the wires is stronger and the contact area larger at a sintering temperature of 1030 °C rather than at 950 °C, for identical gas compositions and sintering times. Stronger and better contact between the wires is of paramount importance in enhancing the thermal performance and system stability, as well as for ensuring the mechanical stability of the bond over time. Top and side views of the finished sintered wire screen have previously been presented in reference [3].

The finished test sample had a sandwich structure as illustrated in Figs. 4 and 8, and consisted of three parts: two 10 mm square, pure solid copper pieces each 5 mm thick; with a 10 mm square, either a multilayered stack or single layer of sintered isotropic copper wire screen in the middle. Two holes, 5 mm deep and 1 mm in diameter, were drilled in to the center of the copper from the side. Special limit of error (SLE) K-type thermocouples then were soldered into these two holes to monitor the bulk temperatures of the copper blocks.

The test articles were fabricated in two steps: first, the required number of layers of isotropic copper mesh were sintered together to obtain the desired volumetric porosity and thickness; and then, the sintered capillary wick structure was carefully cut into a 10 mm by 10 mm square and covered by two 5 mm thick solid pure copper plates. A stainless steel fixture was used to accurately position each part during the final sintering step.

4. Physical models

Both parallel and series methods were used in the current investigation. The unit cell used to develop the physical model of the effective thermal conductivity of sintered

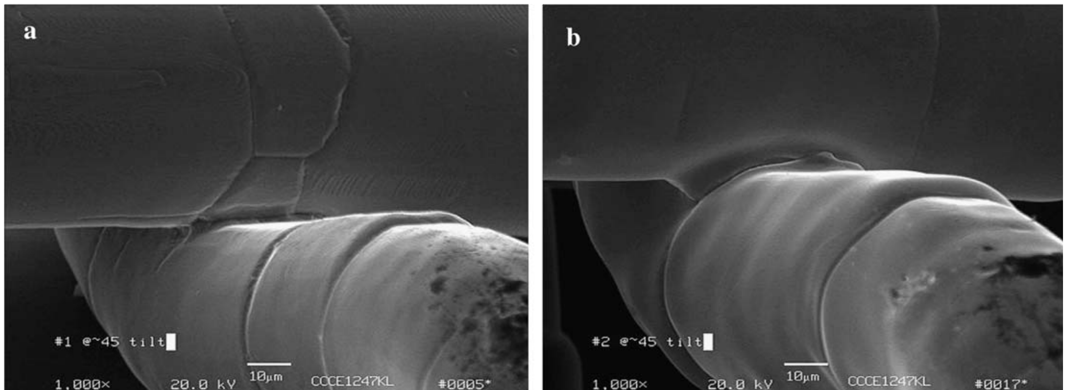

Fig. 3. (a) Contact conditions between wires that are sintered at 950 °C; (b) sintered at 1030 °C for 2 h with gas protection (75% He and 25% H_2).

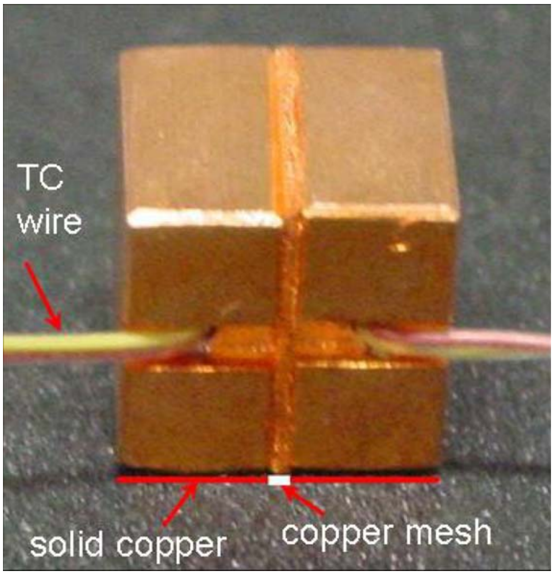

Fig. 4. Test article.

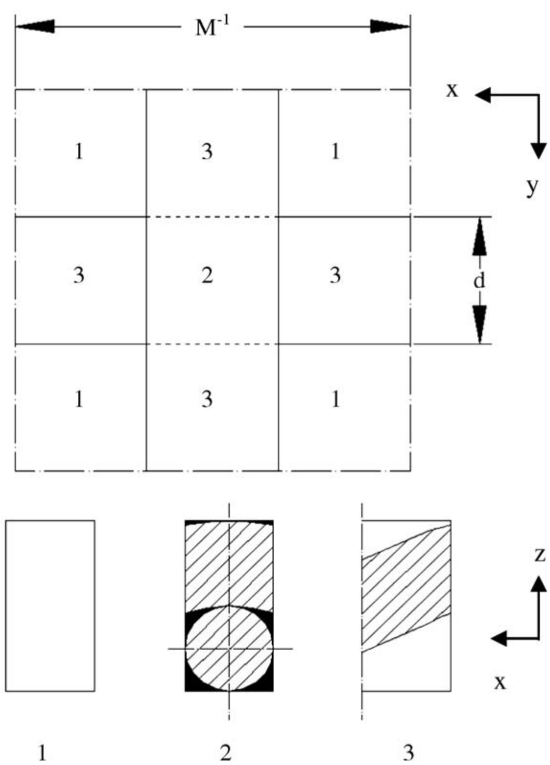

Fig. 5. Schematics of the unit cell and Sections 1–3 denote the pure fluid section; the pure solid metal section; and the fluid and solid metal parts in series, respectively.

wire screen in the z-direction is illustrated in Fig. 5, with the geometric parameters illustrated in Fig. 6.

4.1. Single layer/inline stacked structure

As illustrated in Fig. 5, Section 1 is a pure fluid and because of the minimal thickness of the liquid, the effective thermal conductivity can be treated as a solid with a thermal conductivity equal to that of the fluid. As illustrated in Fig. 3(b), the contact area between wires in Section 2 can be anywhere between zero and the maximum value of d^2. Because an optimal sintering process was used in the current investigation a value of d^2 was assumed [3], and as a result, Section 2 can be treated as a pure solid with a thermal conductivity equal to that of the wire material. Section 3, however, consists of a combination of the solid metal and fluid in series and for this section, the effective thermal conductivity can be expressed as:

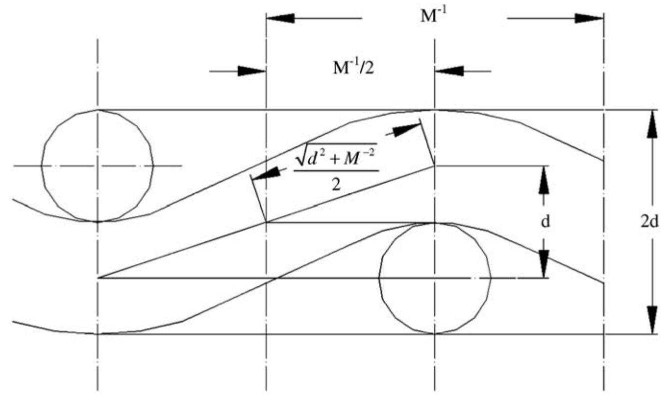

Fig. 6. Geometric relationship of unit cell.

$$K_3 = (\varepsilon_{2s}/K_s + \varepsilon_{2f}/K_f)^{-1} \tag{16}$$

Based on this analysis, Sections 1 and 3 can be represented as individual resistances in parallel and the effective thermal conductivity in the z-direction of a single layer or a layer of inline stacked sintered wire screens can be expressed as:

$$K_{eff} = \varepsilon_1 K_1 + \varepsilon_2 K_2 + \varepsilon_3 K_3 \tag{17}$$

Here $K_1 = K_f$, $K_2 = K_s$ and ε_1, ε_2, and ε_3 can be estimated from the geometrical parameters of the mesh, which are shown as Fig. 6, and can be expressed as,

$$\varepsilon_1 = (1 - Md)^2 \tag{18}$$

$$\varepsilon_2 = (Md)^2 \tag{19}$$

$$\varepsilon_3 = 2Md(1 - Md) \tag{20}$$

where ε_{2s} and ε_{2f} are the relative volumetric porosities of the solid metal and the fluid in Section 2, respectively. These can be computed using the following two equations:

$$\varepsilon_{2s} = \frac{\pi\sqrt{1+(Md)^2}}{8} \tag{21}$$

$$\varepsilon_{2f} = 1 - \varepsilon_{2s} \tag{22}$$

Substituting Eqs. (21) and (22) into Eq. (16) yields

$$K_3 = \left[\frac{\pi\sqrt{1+(Md)^2}}{8} \Big/ K_s + \left(1 - \frac{\pi\sqrt{1+(Md)^2}}{8}\right) \Big/ K_f\right]^{-1} \tag{23}$$

and substituting Eqs. (18)–(20) and Eq. (23) into Eq. (17) yields

$$K_{\text{eff}} = (Md)^2 K_s + (1 - Md)^2 K_f + \frac{2Md(1 - Md)}{\frac{\pi\sqrt{1+(Md)^2}}{8} \Big/ K_s + \left(1 - \frac{\pi\sqrt{1+(Md)^2}}{8}\right) \Big/ K_f} \tag{24}$$

As shown in Eq. (24), a theoretical model of the effective thermal conductivity of sintered copper mesh in the z-direction can be written as a function of Md, K_s and K_f. Rearranging allows Eq. (25) to be expressed in dimensionless form as:

$$K_{es} = (Md)^2 + (1 - Md)^2 \frac{K_f}{K_s} + \frac{2Md(1 - Md)}{\frac{\pi\sqrt{1+(Md)^2}}{8} + \left(1 - \frac{\pi\sqrt{1+(Md)^2}}{8}\right)\frac{K_s}{K_f}} \tag{25}$$

where, K_{es} is defined as the ratio of the effective thermal conductivity, and the thermal conductivity of the solid metal wire, i.e., K_{eff}/K_s. From Eq. (25), if the ratio of $K_f/K_s < 0.01$, this expression can be simplified and expressed as:

$$K_{es} = (Md)^2 \tag{26}$$

Close examination of Eq. (26) indicates that the effective thermal conductivity of the wire screen is governed primarily by the conductivity of Section 2, and in particular, the quality of the bond that exists between the solid portions of the wires in contact with each other. This is physically consistent with the findings of Chang [8] and Hsu et al. [9], whose models for cases 5 and 7 predicted a similar trend, with the only difference resulting from the solid-to-solid contact area for the effective thermal conductivity of the wire screen in the z-direction.

4.2. The multilayer staggered structure

As indicated above and illustrated in Fig. 7, the effective thermal conductivity of multilayer staggered structures in the z-direction can be enhanced through a reduction in the overall thickness of the layer or through an increase in the contact area between the individual wires. When only the decrease in the thickness is taken into account, the model can be simplified as shown in Eq. (27) with the known effective thermal conductivity of the inline stacked sintered copper wire screen given by Eq. (25):

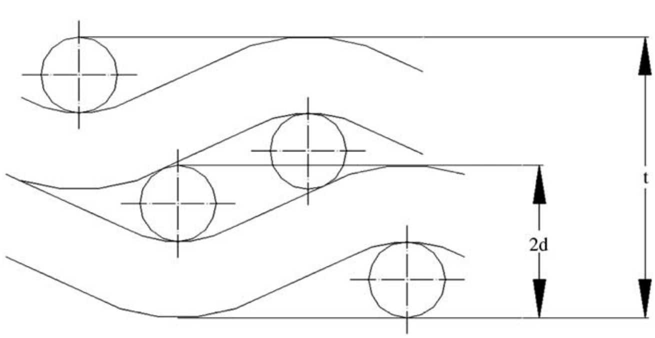

Fig. 7. Geometric relationship of staggered structure.

$$K_{es} = \left\{ (Md)^2 + (1 - Md)^2 \frac{K_f}{K_s} + \frac{2Md(1 - Md)}{\frac{\pi\sqrt{1+(Md)^2}}{8} + \left(1 - \frac{\pi\sqrt{1+(Md)^2}}{8}\right)\frac{K_s}{K_f}} \right\} \Big/ \text{cf} \tag{27}$$

However, the experimental test data in both the current and other investigations are typically much higher than the predictions obtained from Eq. (27). This is not surprising since Eq. (27) does not consider the enhancement resulting from increases in the contact area between the wires. To compensate for this, using a regression analysis an empirical modification constant was developed to represent this enhancement due to the quality of the contact. If the ratio of $K_f/K_s < 0.01$, this value is 1.42 and the model for the staggered structure can be expressed as:

$$K_{es} = 1.42(Md)^2/\text{cf} \tag{28}$$

where the range of cf is governed by the geometric limitations

$$\frac{Md}{\sqrt{Md^2 + 1}} \leqslant \text{cf} \leqslant 1 \tag{29}$$

4.3. Volumetric porosity model

Based on the unit cell illustrated in Fig. 5 and the geometric relationships shown in Fig. 6, the volumetric porosity of the wire screen can be derived as:

$$\varepsilon = 1 - \frac{Md\sqrt{1 + Md^2}}{4\text{cf}} \tag{30}$$

where, cf is the compression factor, where cf = 1 represents a single layer and inline stacked structures; and cf < 1 denotes staggered structures.

5. Experimental facility and calibration process

Two methods are generally employed to measure thermal conductivity in these types of structures: one, a transient method and another one, a steady-state method. In the current investigation, a steady-state method was used to obtain the effective thermal conductivity of individual or multiple layers of sintered copper wire screens. A schematic of the experimental test facility is illustrated in Fig. 8. This test facility is comprised of a heating and cooling system, a position adjusting system, the thermal insulation, and a data acquisition system. The heating system consists of an electric heater and a 10 mm × 10 mm square copper heating block with a 25.4 mm (1 inch) diameter cylindrical portion. Four holes, each 5 mm deep and 1 mm in diameter, were drilled into the center of the copper

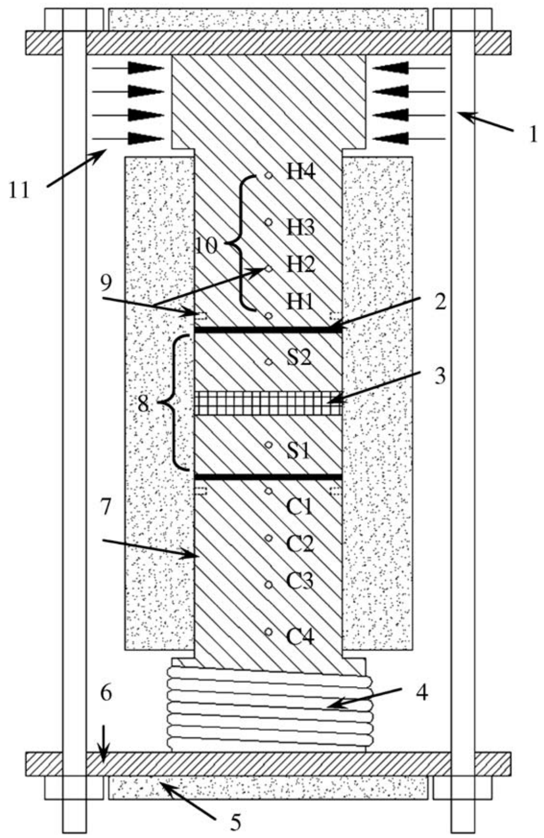

Fig. 8. Schematics of thermal conductivity test setup. 1. Fast bolt, 2. Indium foil, 3. Sintered copper wire screen, 4. Cooling coil, 5. Thermal insulation layer, 6. Al plate, 7. Pure copper bar for heating and cooling, 8. Test article, 9. Holes for thermocouples, 10. Thermocouple group for estimation of heat flux, 11. Heat input.

bar at 10 mm intervals along the length of the heating/cooling blocks. Special limit of error (SLE) K-type thermocouples, were soldered into each hole. Using the temperature difference between thermocouples and the thermal conductivity of the pure copper heating section, the steady-state 1D axial heat flux could be accurately estimated. Heat input was provided from the top and the heat was removed from the bottom portion. In this way, the effects of natural convection occurring in the fluid saturated sintered copper wire screen could be reduced. Indium foil, 0.4 mm thick was placed between the test article and the heating/cooling copper bar to improve the contact thermal conditions.

The contact conditions between the test article and the heating/cooling could be adjusted by the four screws, which connected the top and the bottom aluminum plates. These contact conditions were determined by four K-type thermocouples, located near the surfaces of both the heating and cooling bars and shown as holes near the indium foils in Fig. 8. The optimal contact between the test article and the heating and cooling bars result in a uniform thermal contact resistance, and hence a uniform temperature distribution on the end of the heating and cooling bars as represented by these thermocouples, with identical temperature readings from these thermocouples indicating a parallel and even contact.

The experimental test facility was calibrated by measuring the thermal conductivity of a solid, pure copper cube, 10 mm on a side. The effectiveness of the sintering process could be ascertained by measuring the effective thermal conductivity of a sintered copper bar consisting of two 10 mm square, 5 mm thick bars. The results of these two tests have been presented, discussed and compared previously [3] and demonstrated that the sintering system was capable of obtaining near perfect contact conditions, resulting in an experimental method that was highly accurate and reliable [3].

6. Data reduction and measurement uncertainties

Estimation of the thermal conductivity for this type of situation requires three parameters: the temperature difference across the sample, ΔT; the steady-state heat flux, q''; and the thickness of the sintered copper wire screen layer, t. With these three parameters, the effective thermal conductivity, K_{eff}, of the wire screen in the z-direction can be estimated from Fourier's law.

$$q'' = \frac{K_{\text{Cu}}}{2}[(T_{\text{h4}} - T_{\text{h1}})/4t_{\text{hole}} + (T_{\text{c1}} - T_{\text{c4}})/4t_{\text{hole}}] \tag{31}$$

$$\Delta T = T_{\text{s2}} - T_{\text{s1}} - q''t_{\text{Cu}}/K_{\text{Cu}} \tag{32}$$

$$K_{\text{eff}} = q''t_{\text{mesh}}/\Delta T \tag{33}$$

where, h1–h4 and c1–c4 denote the thermocouple numbers on the heating and cooling sides, respectively. The distance between the two thermocouple holes is represented by t_{hole}, t_{Cu} is the copper thickness between the two holes located on the centerline of the solid copper side of the test sample, as illustrated in Fig. 8, and t_{mesh} is the thickness of the sintered wire screen. In Eq. (31), $K_{\text{Cu}}(T_{\text{h4}} - T_{\text{h1}})/4t_{\text{hole}}$ and $K_{\text{Cu}}(T_{\text{c1}} - T_{\text{c4}})/4t_{\text{hole}}$ denote the heat flux from the heated and cooled ends, respectively, and the mean value is the 1-D axial heat flux through sintered copper wire screen. For each sample, four points at different heat fluxes were used to determine the effective thermal conductivity, and then the averaged value was used as the final effective thermal conductivity of the sample.

The uncertainties of the temperature measurements, the length (or width) and the mass are ±0.4%, 0.001 mm and 0.1 mg, respectively. A Monte Carlo error of propagation simulation indicated the following 95% confidence levels for the computed results: the effective thermal conductivity was less than ±5 W/mK; the temperature difference across the sample, ΔT, was less than ±0.7 K and the porosity, ε, was less than ±1.5%.

7. Results and discussion

7.1. The effective thermal conductivity of sintered copper wire screen

The results of the effective thermal conductivity from the current model and test data are presented in Fig. 9. For

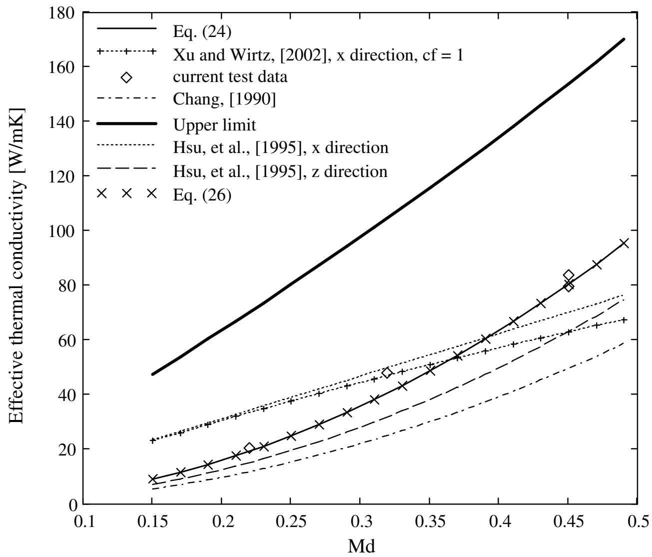

Fig. 9. Effective thermal conductivity from the current model and test data as well as comparisons with existing models for single layer or inline stacked structures.

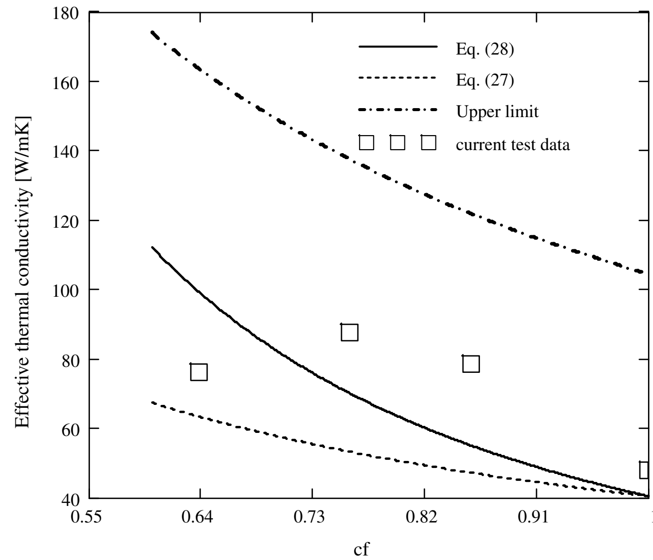

Fig. 10. Effective thermal conductivity as function of cf for staggered structures.

comparison, existing models (the high prediction group) for single layer or inline stacked structures are also plotted in Fig. 9. As indicated in this figure, the values predicted using the present model are higher than the predictions of the models of Chang [8] and Hsu et al. [9] in the z-direction, but the trends are quite similar. One possible reason for this disparity is the variation of the contact area between the wires, which is listed in Table 1. In the current investigation, the contact area between the wires is assumed to be the maximum value, d^2. As indicated, the experimental test data are in reasonably good agreement with the model predictions and indicate that this explanation is reasonable.

Predictions of the effective thermal conductivity of the wire screen in the x-direction obtained from the model of Xu and Wirtz. [2] and Hsu et al. [9] are also shown in Fig. 9 for comparison. The results as determined by Eqs. (24) and (26) are presented in Fig. 9, and clearly indicate that for copper and air, Eqs. (24) and (26) do not differ significantly. These results strongly support the hypothesis that the contact condition between the wires in the z-direction is perhaps the most important parameter in the determination of the effective thermal conductivity of the layers of wire screen.

The effective thermal conductivity of staggered structures is also presented as a function of the compression factor, cf, in Fig. 10. As indicated, Eq. (27) yields predicted values that are somewhat lower than the measured test data. One reason for this is that this expression does not take into consideration the enhancement resulting from the increased contact area between the wires. An empirical constant of 1.42 as shown in Eq. (28) can be derived using a regression technique to compensate for this effect and can then be used to accurately represent the resulting improvement.

7.2. The volumetric porosity of sintered copper wire screen

Predictions based upon the present model and experimental data for a number of different volumetric porosities of sintered copper wire screen are illustrated in Figs. 11 and 12. In Fig. 11, the volumetric porosity is shown as a function of the product of the mesh number and the wire diameter, Md. Comparisons are also made in Fig. 11 with other existing models and experimental test data. The results of this comparison indicate that the predictions from the models appear to be in good agreement when the value of Md is low; however, the values begin to deviate as Md becomes larger. Between all of the models evaluated, the

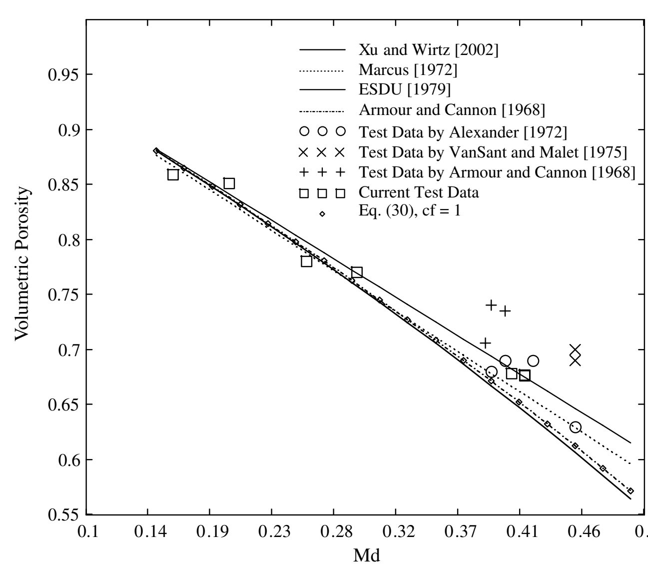

Fig. 11. Volumetric porosity from the current model and test data as well as comparisons with other existing models and test data for single layer or inline stacked structures.

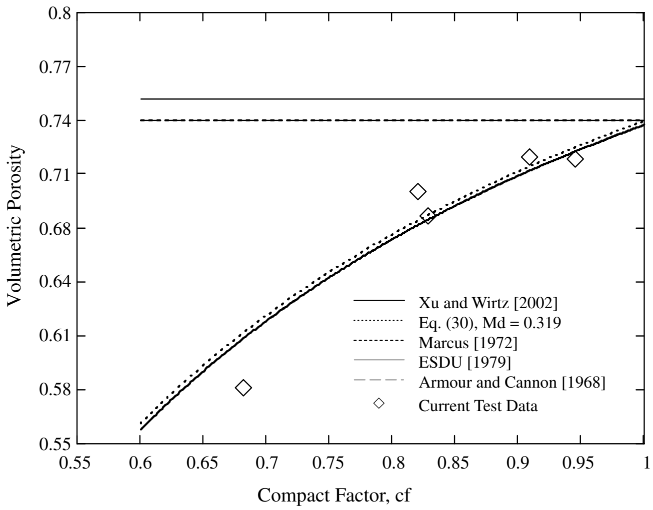

Fig. 12. Volumetric porosity from the current model and test data as well as comparisons with other existing models for staggered structures.

one developed by Xu and Wirtz. [2], as well as Armour and Cannon [13], along with the present model, show the best agreement. Test data from the current investigation agree with these models quite well for large values of *Md*, however, test data from Van Sant and Malet [14] and Armour and Cannon [13] are higher than any of the values predicted by any of the models. One possible reason is that an air gap may exist between the wires for high values of *Md* without any sintering or soldering.

In Fig. 12, the results of the variation in the volumetric porosity for staggered wire screen are shown as a function of the compression factor, cf. As shown, the model of Xu and Wirtz [2] and the present model are in good agreement with the experimental results and with each other. Experimental data covering a wide range of compression factors are also presented and show good agreement with both the model of Xu and Wirtz [2] and the present model.

8. Conclusions

In the current investigation, the information available in the literature on the effective thermal conductivity and volumetric porosity of wire screens were critically reviewed and compared. The existing models and experimental test data indicated that K_{eff} in the x-direction is much higher than in the z-direction. However, some of the cases studied, indicated that high values of K_{eff} in the z-direction could also be obtained if the individual wires are in good contact with one another. In this investigation, a new theoretical model for the effective thermal conductivity in the z-direction is developed, which considers the contact conditions between the wires. It is derived successfully and was verified by experimental test data obtained from the sintered copper wire screens. When the wires are in good contact with one another, the value of the effective thermal conductivity of the wire screen can reach values as high as 4–35% of the thermal conductivity of the metal wire material, with the actual value depending upon the geometric parameter, *Md*, and the physical structure. These results are also strongly supported by comparisons with the existing models. Furthermore, it has been shown that the current approach can be converted to a much simpler form when $K_f/K_s < 0.01$, with the results of this simplified form showing good agreement when compared with the experimental test data of both this and other investigators.

Through this theoretical and experimental investigation, as well as the review of the existing studies of the effective thermal conductivity and volumetric porosity, it is clear that exceptionally high values for the effective thermal conductivity can be achieved for layers of wire screen in both the x- and z-directions, and that the contact conditions between the wires are crucial in determining the magnitude of the effective thermal conductivity in the z-direction.

Acknowledgements

The authors would like to acknowledge the support of the National Science Foundation under award CTS-0312848 and the Office of Naval Research under grant number N00014010454.

References

[1] L. Rayleigh, On the influence of obstacles arranged in rectangular order upon the properties of a medium, Philos. Mag. LVI (1892) 481–502.
[2] J. Xu, R.A. Wirtz, In-plane effective thermal conductivity of plain-weave screen laminates, IEEE TCPT 25 (4) (2002) 615–620.
[3] Chen Li, G.P. Peterson, Yaxiong Wang, Evaporation/boiling on thin capillary wick (I): Thickness effects, ASME J. Heat Transfer, in press.
[4] E.G. Alexander Jr., Structure Property Relationships in Heat Pipe Wicking Materials, Ph.D. Dissertation (1972), Department of Chemical Engineering, North Carolina State University, Raleigh, NC.
[5] J.C.Y. Koh, A. Fortini, Anthony, Prediction of thermal conductivity and electrical resistivity of porous metallic materials, Int. J. Heat Mass Transfer 16 (1973) 2013–2022.
[6] M.I. Aivazov, I.A. Domashnev, Influence of porosity on the conductivity of hot-pressed titaniumnitride specimens, Institute for New Chemical Problems, Academy of Sciences of the USSR. Translated from Poroshkovaya Metallurgiya 8 (9) (1968) 51–54.
[7] R.P. Tye, An experimental investigation of the thermal conductivity and electrical resistivity of three porous 304L stainless steel 'Rigimesh' material to 1300 K, NASA CR 72710 (1970).
[8] W.S. Chang, Porosity and effective thermal conductivity of wire screens, ASME J. Heat Transfer 112 (1990) 5–9.
[9] C.T. Hsu, K.W. Wong, P. Cheng, Effective stagnant thermal conductivity of wire screens, AIAA J. Thermophys. 10 (3) (1995) 542–545.
[10] A.E. Scheidegger, The physics of flow through porous media, University of Toronto Press, Toronto, Ont., CA, 1963, p. 10.
[11] B.D. Marcus, Theory and design of variable conductance heat pipes, NASA CR-2018 (1972).
[12] ESDU, Heat pipes-properties of common small-pore wicks, Data Item No. 79013, Engineering Sciences Data Unit, London, United Kingdom, (1979).
[13] J.C. Armour, J.N. Cannon, Fluid flow through woven screens, AIChE J. 14 (3) (1968) 415–420.
[14] J.H. Van Sant, J.R. Malet, Thermal conductivity of some heat pipe wicks, Lett. Heat Mass Transfer 2 (1975) 199–206.